Available online at www.sciencedirect.com

ScienceDirect

Procedia CIRP 89 (2020) 110–115

www.elsevier.com/locate/procedia

CIRP BioManufacturing Conference 2019

Electrospinning of Poly(vinyl alcohol)-Graphene oxide aligned fibers

P. Ginestra[a*], L. Riva[a], A. Fiorentino[a], D. Zappa[b], E. Comini[b], E. Ceretti[a]

a Department of Mechanical and Industrial Engineering, University of Brescia, Via Branze 38, 25123, Brescia, Italy.

bDepartment of Information Engineering, University of Brescia, Via Branze 38, 25123, Brescia, Italy.

* Corresponding author. Tel.: +390303715584; E-mail address: paola.ginestra@unibs.it

Abstract

Electrospinning is a well know technology for the production of nano and micro fibers. Graphene has been used in different fields due to its unique stability. Reduced graphene oxide (rGO) is prepared from the reduction of graphene oxide. In this work, we electrospun of Polyvinyl Alcohol (PVA) solutions with rGO to combine the different physical properties of the materials, on a rotating collector to verify the influence of the solutions and rotation on the morphology of the fibers. The optimization of the process highlighted the influence of the flow rate and tip-collector distance in relation to the rotation speed used.

Keywords: electrospinning, graphene, polymers.

1. Introduction

The electrospinning technique is a widespread used technology for the production of nano and micro fibers for several applications including wearable smart tissues, sensors and tissue engineering. The electrospinning technique is largely employed in the biomedical field because almost all the tissues and organs (i.e. skin, collagen, cartilage and bone) show a structure very similar to nanosized fibrous structures. Hence, researches are focused on the generation of fibrous scaffolds for tissue engineering, drug delivery mechanisms and wound dressing.

Biocompatible and biodegradable fibrous scaffolds are preferred over conventional scaffolds in the regeneration of tissues, because of the ability in mimicking the extracellular matrix [1,2,3]. Therefore, electrospun nanofibers show a great cell growing capability. In particular, nanofibrous networks of aligned fibers can promote and guide the orientation of the cells supporting their differentiation and maturation. In addition to that, bio/natural polymers are characterized by an excellent biocompatibility and biodegradability, a primary feature for tissue engineering [4,5].

Different techniques have been combined with the electrospinning traditional set-up to modify and control the deposition and the morphology of the fibers [6]. Among the usage of parallel electrodes to collect crisscrossing nanofibers, rotating collectors are preferable to fabricate aligned fibrous mats with tailorable thickness and width. The rotation speed of the drum is found to be the most important parameter to influence the alignment of the fibers due to the mechanical stretching forces that affect the ejected solution [7,8]. Graphene has been largely used in different technological fields due to its unique properties [9,10]. In particular, graphene has fundamental thermal, mechanical, electrical and thermoelectric properties so it is often mixed within a polymer matrix to obtain a homogeneous dispersion. Polyvinyl Alcohol (PVA) is a water-soluble, biodegradable, non-toxic polymer characterized by good stability and

10.1016/j.procir.2020.05.126

physical properties. Reduced graphene oxide (rGO) is prepared from the reduction of graphene oxide (GO) by thermal, chemical or electrical treatments; in particular rGO can be produced by removing all the oxygen functional groups from GO. In order to improve the performances of graphene-based nanocomposites, a full exfoliation and complete dispersion of the graphene nanofiller in the matrix is crucial. However, due to the dimension and shape of the graphene sheets, irreversible agglomerates tend to be developed. In addition to that, graphene is a hydrophobic material, so its applications in aqueous-based preparations are limited. PVA has some disadvantages such has weak mechanical properties and thermal stability but can be combined with graphene to enhance these properties [11]. The possibility of incorporating graphene and its derivatives in nanofibers leads to better thermal and electrical conductivities of the networks. In the preparation of the electrospinning solution, the interactions between the polymer and graphene, such as hydrogen bonds, affect the solution viscosity, conductivity and rheology [12].

In this work, we focused on the electrospinning tests of a PVA-rGO solution on a rotating collector to verify the influence of the collector rotation speed on the morphology and distribution of the resulting fibers compared to the electrospinning tests carried out on a square flat collector.

2. Electrospinning tests

PVA (Mw 89.000-98.000, 99+% hydrolyzed) and reduced Graphene Oxide (rGO) (1%, stabilized with poly(sodium 4-styrenesulfonate, 10mg/ml, dispersion), were purchased from Sigma-Aldrich Chemistry. The electrospinning parameters used in the following tests were set in relation to the literature on electrospinning tests performed on synthetic polymers [6,14], polymer-graphene solutions [10,11] and rotating drums usage for the fibers collection [7,8].

2.1. Electrospinning on flat collector

A solution of 15% PVA and the solution of 1% of rGO were mixed at room temperature. A solution of 3:2 ratio of PVA: rGO was prepared, stirred for 2 hours and poured into a 10 ml syringe equipped with G21 mm needle. The electrospinning equipment is reported in Fig. 1. The flow rate was set to 1 ml/h and the voltage was set at 20 kV. The fibers were collected on the square flat collector by varying the distance from the tip to the collector between 20mm and 80mm.

2.2. Electrospinning on rotating drum

The solution electrospun on a flat collector was tested on a rotating drum collector to verify whether the rotation of the collector could affect the diameter and the alignment of the fibers (Fig. 2).

The designed collector was properly integrated in the electrospinning equipment as reported in Fig. 3.

Fig. 1. Electrospinning set-up integrated with the flat square collector.1) syringe pump, 2) needle tip, 3) collector.

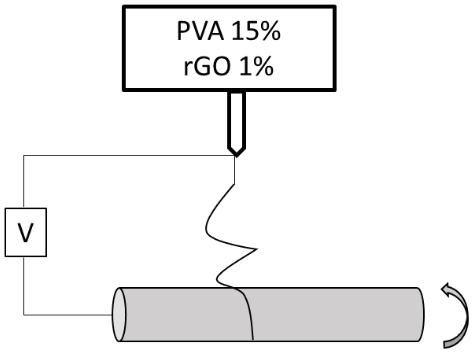

Fig. 2. Scheme of the electrospinning process on the rotating drum.

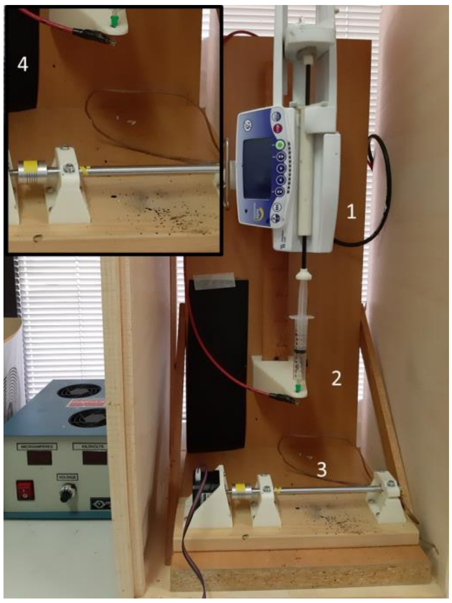

Fig. 3. Electrospinning set-up integrated with the rotating drum collector. 1)syringe pump, 2) needle tip, 3) collector, 4) zoom on the tip-collector distance.

In this case, three replicas for each electrospinning test were carried out by varying the tip-collector distance, the flow rate and the rotation speed of the collector as summarized in Table 1.

Table 1. Designed electrospinning tests.

Parameter	Range	Set value
Tip-collector distance [mm]	20-120	20, 80
Voltage [kV]	0-20	20
Flow Rate [ml/h]	0.1-1	0.5, 1
Rotation speed [rpm]	0-300	100, 200

3. Fibers characterization

The electrospun samples surface was observed using the Zeiss LEO 1525 scanning electron microscope (SEM). The measurements of the diameters and alignment of the fibers were calculated while processing the images with the ImageJ imaging software [13].

3.1. rGO-PVA fibers

The morphology of the samples is reported in Fig. 4. At low distance the solvent is not able to completely evaporate and this is testified by the presence of watery fibers and beads. This leads to the formation of irregular fibers due to the presence of the beads and so the technique can be compared to electrospray. The proximity between the tip and the collector is characterized by an electric field that leads to the surface tension charge distortion which causes a difficulty in the evaporation of the solvent.

When the distance is increased, the quality of the fibers gets better: they are more defined and the fibrous mat is thicker (Fig.4).

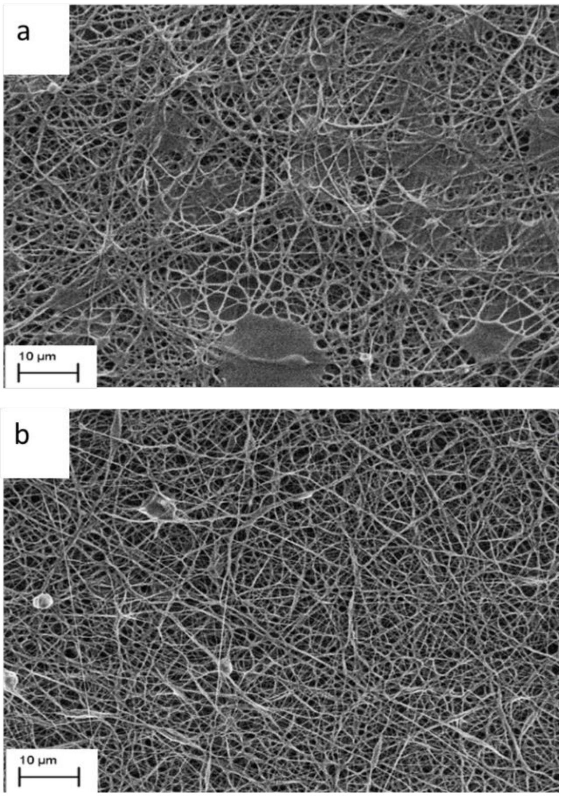

Fig. 4. SEM images of PVA-rGO fibers electrospun at a tip-collector distance of (a) 20 mm and (b) 80 mm on the flat square collector.

The results of the fibers measurements are reported in the histograms of Fig. 5 and in Table 2. The variability of the data is higher as the tip-collector distance is reduced due to a less control on the electric field at lower distances. Considering the dimensions of the fibers, the distances of electrospinning are slightly influencing the diameter of the collected fibers. In particular, the diameter of the fibers is lowered when the tip-collector distance is increased as expected from these type of tests [14], but the difference is not significant confirming the influence of the polymer concentration on the morphology of the fibers that leads to a reduced variation of the fibers due to the presence of the graphene.

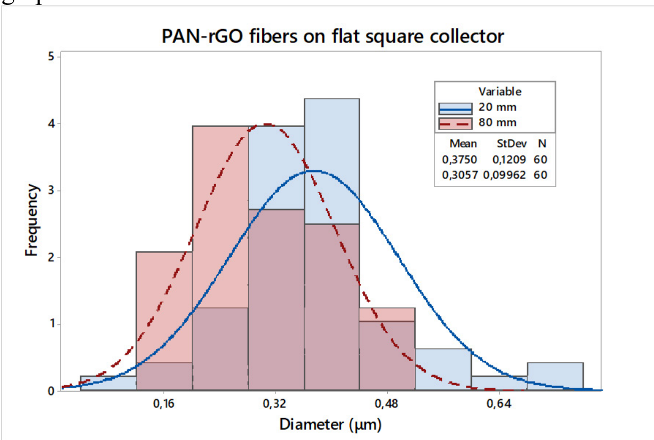

Fig. 5. Histograms of the frequency of the diameter of PVA-rGO fibers electrospun at a tip-collector distance of (blue) 20 mm and (red) 80 mm on the flat square collector.

Table 2. Results of the measurements of the PVA-rGO fibers on the flat square collector.

Flow rate (ml/h)	Tip-collector distance (mm)	Fibers diameter (µm)
1	20	0.38±0.1
1	80	0.3±0.1

3.2. rGO-PVA fibers on rotating drum

The images of the samples electrospun on the rotating drum at a speed of 100 rpm are reported in Figure 6.

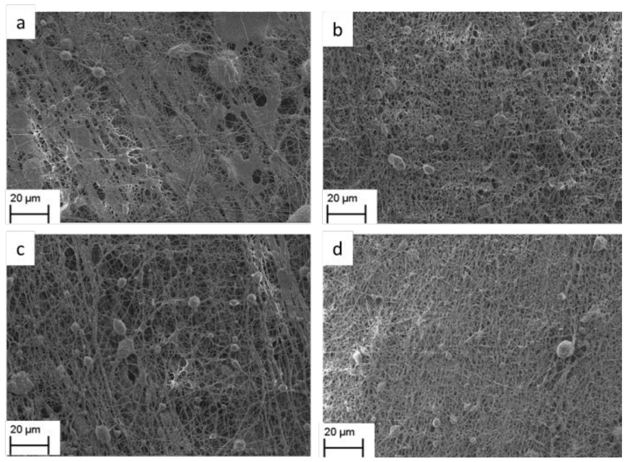

Fig. 6. SEM images of PVA-rGO fibers electrospun at a tip-collector distance of 20 mm (a-c) and 80 mm (b-d) on the rotating drum collector at 100 rpm. Samples a and b are electrospun at 0.5 ml/h while c and d at 1 ml/h.

As shown from the pictures, no significant trend is visible in relation to the alignment of the fibers due to the presence of the rotating drum. As a matter of fact, from Fig. 6a, it is possible to recognize a preferential direction of the fibers that is not evident for the other electrospinning configurations.

In this case, the uniformity of the fibers distribution on the collector is higher when the electrospinning distance is increased independently from the flow rate used (Fig. 7). The diameter of the fibers is lowered when a flow rate of 0,5 ml/h is used in both cases of tip-collector distances of 20 mm and 80 mm. Moreover, at a tip-collector distance of 20 mm the difference between the diameter of the fibers at different flow rates is less evident due to the inadequate evaporation of the solvent that causes the presence of beads and flat fibers. These structures can act as agglomerates from which the electrospun fibers are formed. Compared to the fibers collected on the flat collector, an increase of the diameter is measured at lower flow rates confirming that the behavior of the fibers is more influenced by the collector used than by the electrospinning parameters. In particular, the fibers collected by the effect of the rotation speed are thicker due to the action of stretching that tends to overlap the fibers and spread the agglomerates.

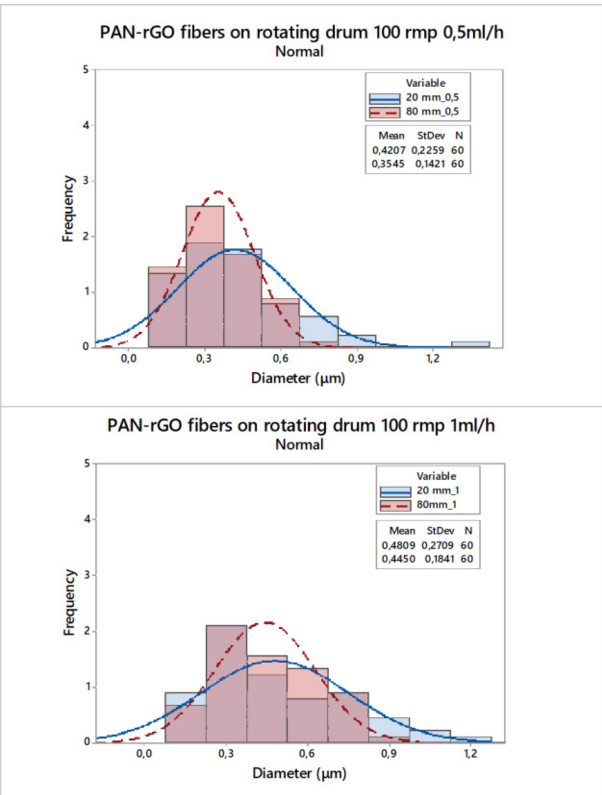

Fig. 7. Histograms of the frequency of the diameter of PVA-rGO fibers electrospun at a tip-collector distance of (blue) 20 mm and (red) 80 mm on the rotating drum collector at a speed of 100 rpm.

The samples electrospun on the rotating drum at a speed of 200 rpm are shown in Fig 8. Figure 8 shows a clear alignment of the fibers in the direction of the rotating drum rotation. The fibers electrospun at a tip-collector distance of 20 mm are more aligned compared to the fibers collected at a distance of 80 mm. This result is probably due to the higher effect of the rotation when the fiber is produced from the Taylor cone [15] by the electric field. Although, the diameter of the fibers is increased compared to the flat collector configuration due to the melting of the aligned fibers along the rotation direction.

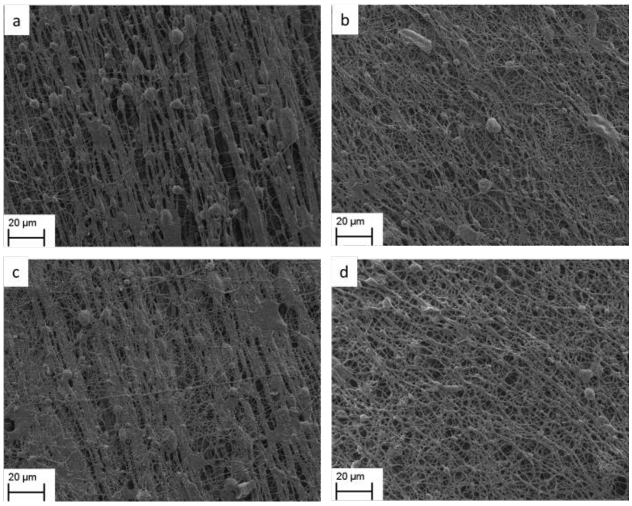

Fig. 8. SEM images of PVA-rGO fibers electrospun at a tip-collector distance of 20 mm (a-c) and 80 mm (b-d) on the rotating drum collector at 200 rpm. Samples a and b are electrospun at 0.5 ml/h while c and d at 1 ml/h.

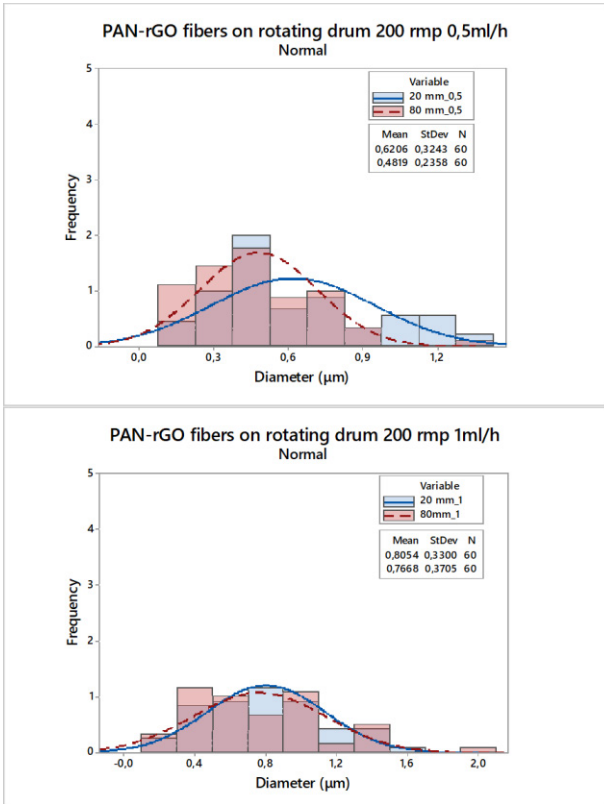

Fig. 9. Histograms of the frequency of the diameter of PVA-rGO fibers electrospun at a tip-collector distance of (blue) 20 mm and (red) 80 mm on the rotating drum collector at a speed of 200 rpm.

The histograms in Figure 9 report the evaluation of the dimension of the fibers electrospun with a speed of the drum of 200 rpm. In this case, the diameters of the fibers are higher compared to the results of the tests performed at 100 rpm in relation to all the parameters configurations. The higher rotation speed leads to stronger dragging forces acting on the produced fibers causing an overlapping of the fibers that are melting following the rotation direction. The diameter of the fibers tends to increase when the tip-collector distance is decreased as reported for the tests at 100 rpm. In this case, at a flow rate of 1ml/h the distribution of the fibers is more uniform in relation to the electrospinning distance considered. The summarized dimensions of the fibers depending from the electrospinning parameters on the rotating collector are reported in Table 3.

Table 3. Results of the measurements of the PVA-rGO fibers on the rotating drum.

Rotation speed (rpm)	Flow rate (ml/h)	Tip-collector distance (mm)	Fibers diameter (µm)
100	0.5	20	0.42±0.2
100	0.5	80	0.35±0.1
100	1	20	0.48±0.3
100	1	80	0.44±0.2
200	0.5	20	0.62±0.3
200	0.5	80	0.48±0.2
200	1	20	0.80±0.3
200	1	80	0.76±0.4

3.3. Alignment of the rGO-PVA fibers

To confirm what shown by the images, the fibers orientation was measured processing the SEM pictures (Fig. 8) with ImageJ and taking 30 measures from each sample. Then, the frequency distributions of the fibers orientation (Fig. 10 and 11) were used to evaluate the influence of the rotation of the drum on the mats.

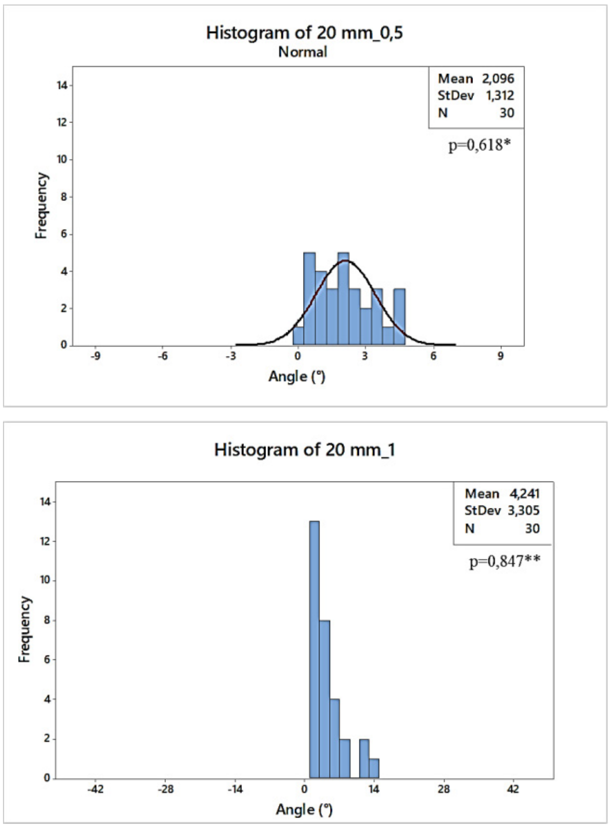

Fig. 10. Histograms of the frequency distributions of the fibers orientation on the samples electrospun at a tip-collector distance of 20mm at 200 rpm. *Box-Cox transformation: λ = 0,5; **Johnson transformation.

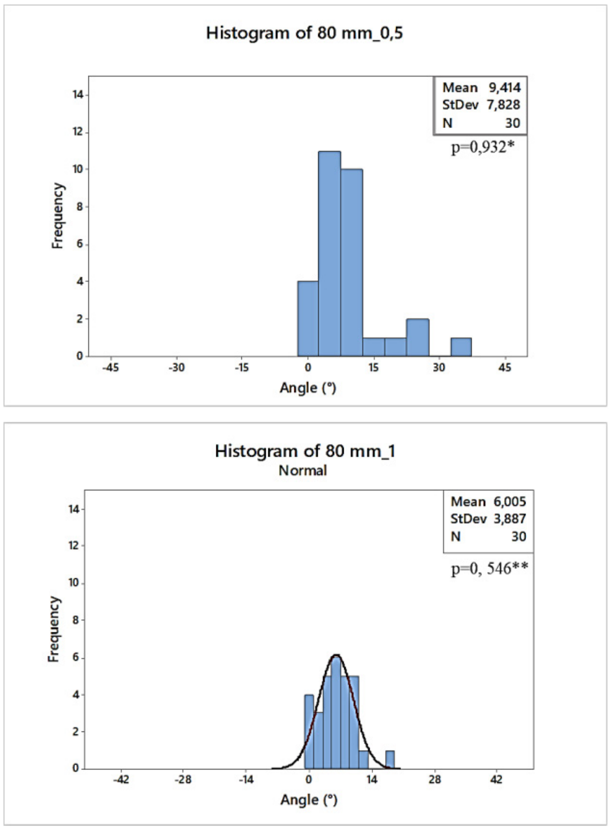

Fig. 11. Histograms of the frequency distributions of the fibers orientation on the samples electrospun at a tip-collector distance of 80mm at 200 rpm. *Johnson transformation; ** Box-Cox transformation: λ = 0,5.

Results show that a predominant orientation of the fibers is recognizable for all the configurations. In particular, considering the reference angle of the drum rotation direction (0°) the calculated maximum variance of the fibers orientation is within 10 degrees in relation to the main direction. Moreover, when the single configurations are compared, it is possible to observe that:

- Tip-collector distance of 20 mm: the fibers show an orientation along the rotation direction but when a flow rate of 1ml/h is used, the variability of the data increases due to the deposition of fibers randomly oriented through the aligned mats.
- Tip-collector distance of 80 mm: the fibers do not show any significant trend when a flow rate of 0.5 ml/h is used while a main direction with a lower standard deviation is observed at a flow rate of 1 ml/h.

A tip-collector distance of 20mm is therefore the most effective in controlling the fibers orientation. On the other hand, at this distance, the fibers are overlapped and melted together due to a poor evaporation of the solvent. If the electrospinning distance is increased to 80 mm, the orientation of the fibers is more uniform at a flow rate of 1ml/h where the linear velocity of the rotating cylinder surface matches with the evaporating jet deposition. In this case, the fibers are almost randomly oriented at a lower flow rate. This is probably due to the rotation speed that can cause fiber fractures and turbulent air flow around the perimeter of the rotating collector.

4. Conclusions

In this paper, the manufacturing process to produce aligned fibers from polymer-graphene water-based solutions via electrospinning on a rotating drum is proposed. A comparison between the fibers deposited on a flat square collector and on the rotating drum showed that the fibers deposited due to the rotation of the collector are characterized by a bigger diameter due to the overlapping of the fibers and the spreading of the agglomerates typical of the water-based solutions. Moreover, at low tip-collector distances the inadequate evaporation of the solvent leads to the formation of flat fibers and beads causing a higher variability of the data. The rotation speed of the collector is influencing the alignment of the fibers according to the direction of the rotation. In particular, a speed of 100 rpm is not allowing the stretching of the fibers that are randomly deposited. When the rotation speed is increased to 200 rpm the fibers are collected accordingly to the rotation of the drum showing a uniform alignment on the main direction. At lower electrospinning distances, the alignment is also causing a partial overlapping of the fibers that result flat and with higher diameters compared to the fibers collected on the flat collector. Furthermore, a flow rate of 0.5 ml/h is probably too low and the rotation can break the fibers at higher rpm. Finally, the evaporation of the solvent is a crucial factor for the variability of the fibers alignment as showed by the uniform distribution of the fibers when a distance of 80 mm and a flow rate of 1 ml/h is adopted. To summarize the outcomes of this work, the best parameters for the obtainment of aligned fibers with a rotating drum found for this electrospinning configuration and the used PVA-rGO solution are reported in Table 4:

Table 4. Parameters for the obtainment of aligned fibers.

Parameter	Value
Tip-collector distance [mm]	20
Voltage [kV]	20
Flow Rate [ml/h]	0.5
Rotation speed [rpm]	200

References

[1] Ginestra PS, Pandini S, Fiorentino A. et al. Microstructured scaffold for guided cellular orientation: Poly(ε-caprolactone) electrospinning on laser ablated titanium collector. Cirp Journal of Manufacturing Science and Technology. 2017; 19: 147-157.

[2] Dias JR, Santos C, Horta J, Granja PL and Bártolo, PJ. A new design of an electrospinning apparatus for tissue engineering applications. International Journal of Bioprinting. 2017; 3(2): 1-9.

[3] Buenrostro CM, Gomar , Scalmana M, Ortega W and Rodriguez C. Study of parameters in electrospun fibers for tissue engineering applications. 2nd International Conference on Design and Processes for Medical Devices, Monterrey, Mexico 2014.

[4] Geim A.K., Graphene: status and prospects. Science 2009; 324: 1530-1534.

[5] Kakran M., L. Li Carbon nanomaterials for drug delivery. Key Eng Mater 2012; 508: 76-80.

[6] Gomar J, Scalmana M, Buenrostro CM, Ciurana J, Rodriguez C and Ortega W. Design of a scaffold hybrid machine for tissue engineering application. 2nd International Conference on Design and Processes for Medical Devices, Monterrey, Mexico 2014.

[7] Long YZ, Yan X, Wang XX, Zhang J and Yu M. Chapter 2 – Electrospinning: The Setup and Procedure. In Ding, Wang and Yu editors. Electrospinning: Nanofabrication and Applications. Micro and Nano Technologies; 2019. p. 21-52.

[8] Yuan H, Zhiu Q and Zhang Y. Improving fiber alignment during electrospinning. In Afshari M. Electrospun Nanofibers. Woodhead Publishing Series in Textiles; 2017. p. 125-147.

[9] Ginestra PS, Ghazinejad M, Madou M, Ceretti E. Fabrication and characterization of polycaprolactone-graphene powder electrospun nanofibers. Proc. SPIE 9932, Carbon Nanotubes, Graphene, and Emerging 2D Materials for Electronic and Photonic Devices IX, 99320A. 2016.

[10] Ceretti E, Ginestra PS, Ghazinejad M, Fiorentino A, Madou M. Electrospinning and characterization of polymer-graphene powder scaffolds. Cirp Annals 2017; 66(1): 233-236.

[11] Lee JKL, Chen N, Peng S. et al. Polymer-based composites by electrospinning: Preparation & functionalization with nanocarbons. Progress in Polymer Science 2018; 84: 40-84.

[12] Wang B, Chen Z, Zhang J, Cao J, Wang S. et al. Fabrication of PVA/graphene oxide/TiO2 composite nanofibers through electrospinning and interface sol–gel reaction: Effect of graphene oxide on PVA nanofibers and growth of TiO2. Colloids and Surfaces A: Physicochem. Eng. Aspects 2014; 457:318–325.

[13] Rasband WS, ImageJ, U. S. National Institutes of Health, Bethesda, Maryland, USA, http://imagej.nih.gov/ij/, 1997-2014.

[14] Ginestra P, Ceretti E, Fiorentino A. Electrospinning of poly-caprolactone for scaffold manufacturing: experimental investigation on the process parameters influence. Procedia CIRP 2016; 49: 8-13.

[15] Chung S and Webster TJ. Antimicrobial nanostructured polyutethane scaffolds. In Afshari M. Advances in Polyurethane Biomaterials. Woodhead Publishing Series in Textiles; 2016. p. 503-521.